

3D DOSIMETRY FOR SELECTIVE INTERNAL RADIATION THERAPY OF UNRESECTABLE LIVER CANCERS USING YTTRIUM-90 LOADED MICROSPHERES: CASE REPORT

Marilyne Kafrouni^{1,2}, Carole Allimant¹, Marjolaine Fourcade¹, Sébastien Vauclin², Alina-Diana Ilonca¹, Fayçal Ben Bouallègue¹, Boris Guiu¹ and Denis Mariano-Goulart¹

¹CHRU of Montpellier
371, avenue du doyen Gaston Giraud
34295 Montpellier cedex 5, France
marilyne.kafrouni@gmail.com

²DOSIsoft SA
45/47, avenue Carnot
94230 Cachan, France
info@dosisoft.com

ABSTRACT

Today, in selective internal radiation therapy (SIRT), activity to inject is planned by standardized approaches that can be easily applied in everyday clinical workflow. However, interest for advanced dosimetry tools is growing since dose-effect relationship has been highlighted in the literature by different studies. This work aims at describing the implementation and potential of 3D voxel-based personalized dosimetry compared to standard approach. This is done through the report of a 68-year-old male patient with liver metastasis from colorectal carcinoma. A whole liver radioembolization using resin microspheres (SIR-Spheres[®], SIRTex, North Sydney, Australia) was performed with a narrow dose constraint of 30 Gy to non-tumoral liver (NTL) to preserve enough hepatic integrity. On one hand, the MIRD-based partition model, considered as standard approach, was applied on the uptake volume defined using Syngo[®].via software solution (Siemens, Erlangen, Germany). On the other hand, both predictive and *in vivo* control dosimetries were carried out using a SIRT treatment planning system (TPS) (PLANET[®] Dose, DOSIsoft, Cachan, France) on anatomical and functional volumes. The standard and TPS calculations estimated an average planned dose to NTL close to 30 Gy. Planned doses to the tumoral liver calculated by the partition model applied at the organ level and by the 3D TPS calculation at voxel level were 118 and 71 Gy respectively. Differences between both methods were partly related to the volume definition. Additional information provided by the TPS allowed to slightly adjust the activity to be injected delivering sufficient dose to tumoral liver while saving NTL as much as possible. *In vivo* dosimetry was performed on ⁹⁰Y quantified PET images with the SIRT TPS and allowed to know the dose delivered to each region. This had an interest for the patient follow-up analysis and to consider later another possible treatment. SIRT TPS seemed to be a clinical decision-making tool thanks to the possible risk/benefit balance optimization. The study will be carried out with further patients to open the way to more personalized SIRT dosimetry.

1. INTRODUCTION

Selective internal radiation therapy (SIRT) is a loco-regional therapeutic option for unresectable primary and secondary liver cancers. Yttrium-90 (⁹⁰Y) loaded microspheres are injected in the hepatic artery and trapped in the tumor microvasculature. ⁹⁰Y is used for its tumoricidal β^- emission with maximum and average β^- energies of 2.28 MeV and 934 keV respectively, a mean range in soft tissue

of 4.1 mm and half-life of 64.2 hours [1]. ^{90}Y also allows PET imaging thanks to its minor positron emission (branching ratio of $31.86 \pm 0.47 \times 10^{-6}$ [2]). In the last few years, many studies have reported ^{90}Y SIRT therapeutic efficacy [3]-[5]. This efficacy is partly related to the unique dual vascular supply of the liver that enables to provide high radiation doses to tumoral hepatic tissue while sparing the surrounding normal liver tissue [6][7].

Internal dose calculation is commonly based on methods easy to apply clinically. Since several studies highlight dose-effect relationship for SIRT [8]-[14], interest is now growing for advanced calculations and dose analysis tools as the ones used in external beam radiation therapy (EBRT).

Today, new systems are available to address these needs. The Nuclear Medicine department of Montpellier University Hospital implemented one of them for treatment planning and *in vivo* dose control purposes. This study reports a clinical case in order to illustrate the potential of 3 dimensional (3D) voxel-based personalized dosimetry compared to standard approach.

2. MATERIALS AND METHODS

2.1. Patient Characteristics

The study reports the case of a 68-year-old male patient with bilobar metastasis from colorectal carcinoma. Four lesions were visible on the magnetic resonance imaging (MRI) exam and are referred in this paper according to their location in the liver: “central” (in the segment I, close to the inferior vena cava), “III” (in the segment III), “V” (in the segment V) and “VII” (in the segment VII).

Therapeutic options were discussed in multidisciplinary staff meeting. The patient had been treated by systemic chemotherapy and intra-arterial chemotherapy. His “central” lesion was unresectable because of its location right next to the inferior vena cava. The decision of whole liver radioembolization was taken.

2.2. SIRT Workflow

2.2.1. The “workup”

First, therapy session was simulated by the planning “workup”. 209 MBq of $^{99}\text{Tc}^{\text{m}}$ -labeled macroaggregated albumin (MAA) were administered in the hepatic artery by an interventional radiologist. Nuclear medicine imaging was done within one hour after the intervention. The aim of the workup was to assess the lung shunt fraction (LSF), the extra-hepatic uptake and the activity of ^{90}Y to inject based on MAA distribution. LSF was evaluated to 0.3% using anterior and posterior planar scans (acquisition parameters: window 140 keV +/- 7.5%, matrix 256 x 256, 5 min, low energy collimator). SPECT/CT data were acquired on a Symbia Intevo system (Siemens, Erlangen, Germany) with the following parameters: window of 140 keV +/- 7.5%, 32 projections, 25s/projection, matrix 128 x 128, voxel size 4.79 mm x 4.79 mm x 4.79 mm, low energy collimator. SPECT data were reconstructed using Flash 3D Iterative Reconstruction (Siemens) with 5 iterations/8 subsets, attenuation and scatter corrections. Data were then visualized and analyzed by the nuclear medicine physician and the medical physicist. The activity to administer was determined using the standard approach and adjusted with the analysis at the voxel level.

2.2.2. Pre-implantation dosimetry at organ level

Dosimetry was first assessed using the partition model, considered in this paper as the “standard approach”. Tumoral liver (TL) and injected liver (IL) uptakes were quantitatively assessed using Syngo[®].via software solution (Siemens, Erlangen, Germany) following Garin *et al.* methodology [15]. In this particular case, the injected liver is the whole liver. The functional TL and IL volumes ($V_{TL\text{-uptake}}$ and $V_{IL\text{-uptake}}$) were delineated using an isocontour method (Figure 1). This was done by adjusting the uptake threshold (% of maximum intensity) making volumes match, visually speaking, with the anatomical boundaries visible on the MRI exam (Figure 2). TL volume was defined on the central lesion uptake. Volumes (V) and their associated number of counts (N) were: $V_{TL\text{-uptake}} = 111$ mL / $N_{TL\text{-uptake}} = 2910$ counts and $V_{IL\text{-uptake}} = 3552$ mL / $N_{IL\text{-uptake}} = 874$ counts

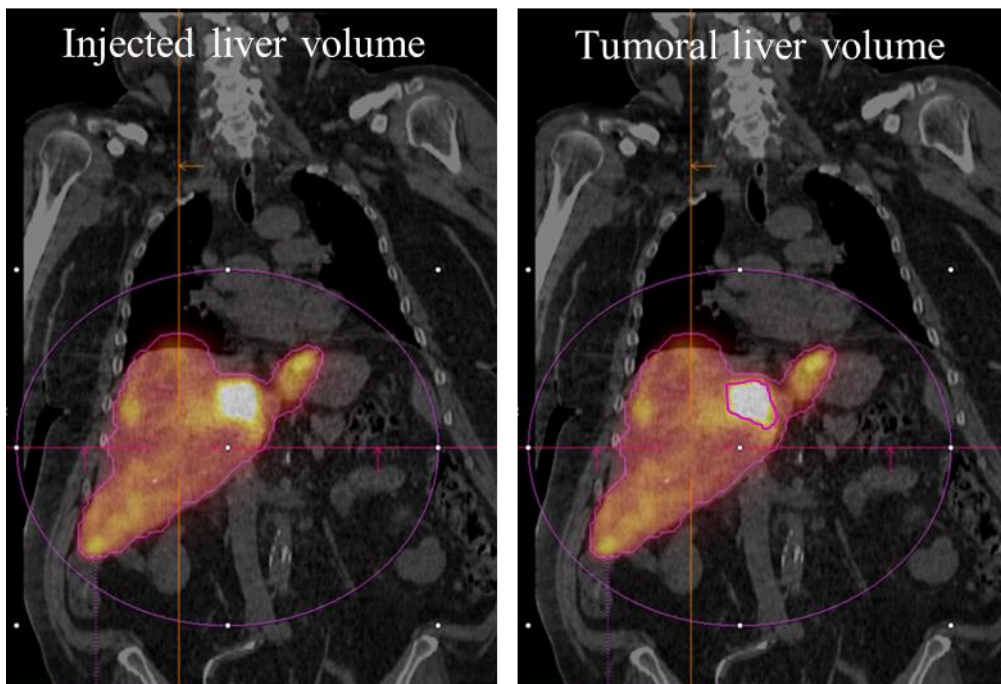


Figure 1: Partition model: IL (on the left) and TL (on the right) volume definition using uptake isocontour (Syngo[®].via, Siemens).

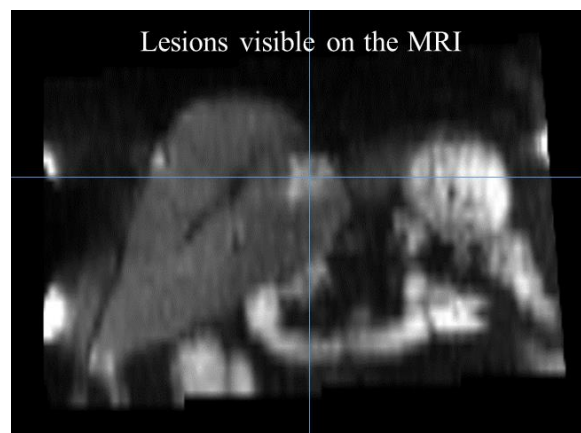


Figure 2: Lesions visible on the diagnostic MRI used as a support for uptake volume definition.

The patient had been recently treated by intensified hepatic intra-arterial chemotherapy with risk of hepatic function damage. In this context, a narrow dose constraint of 30 Gy to non-tumoral liver (NTL) was set to preserve hepatic function as much as possible. The NTL volume was defined as $V_{NTL-uptake} = V_{IL-uptake} - V_{TL-uptake}$.

Based on MAA distribution the planned activity of ^{90}Y to administer was determined according to this 30 Gy constraint by applying the partition model.

Activity and dose to each compartment C (TL and NTL) were calculated by the Medical Internal Radiation Dose (MIRD) formalism [16]:

$$A_C (GBq) = \frac{N_C}{N_{TL} + N_{NTL}} \times A_{to\ inject} (GBq) \times (1 - LSF) \quad (1)$$

$$D_C (Gy) = \frac{A_C (GBq) \times 50}{m_C (kg)} \quad (2)$$

where N_{TL}/N_{NTL} are respectively the counts in the TL and NTL uptake volumes, LSF is the lung shunt fraction (in %), N_C the counts in the compartment, m_C the compartment mass, A_C the compartment activity, D_C the dose to the compartment.

2.2.3. Pre-implantation dosimetry at voxel level

Up to March 2016, dosimetry at Montpellier University Hospital was only performed according to the MIRD-based method as described in the previous section. From this point, dosimetry planning was also conducted using a 3D TPS (PLANET[®] Dose, DOSIsoft, Cachan, France) and following a whole process similar to EBRT (Figure 3).

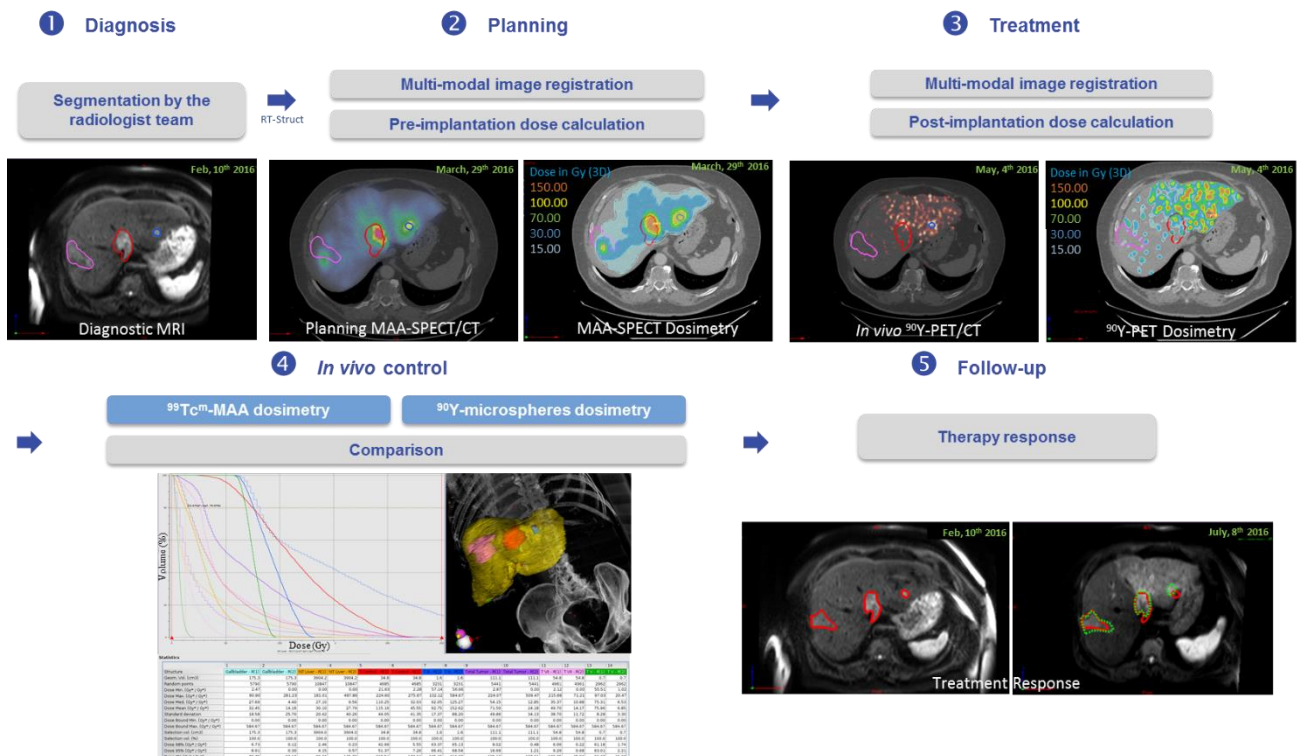


Figure 3: SIRT workflow using a TPS (PLANET[®] Dose, DOSIsoft). Three lesions are visible in the slice chosen here: VII (pink), central (red) and III (blue). The tumor VII MAA uptake is not significant in this particular slice but this lesion was targeted.

The first step was the anatomical segmentation by the radiologist of the whole liver and TL volumes on MRI scan using the diagnostic workstation available in the radiology department (AW Workstation, GE Healthcare, Waukesha, WI, USA). Contours were then imported as RT-Structure set format in the 3D TPS. Then, multimodality image registration allowed to get the contours from MRI exam to the MAA-SPECT/CT space and sampling. In the clinical context of this patient, the gallbladder and the NTL anatomical volumes (respectively $V_{gallbladder-anat}/V_{NTL-anat}$) were also segmented using the TPS. In this case (whole liver treatment), the anatomical NTL volume was defined by subtracting the anatomical TL volume (sum of the 4 lesions) to the whole liver volume.

3D Dose calculation was then performed using a kernel convolution algorithm at voxel level as described by Dieudonné *et al.* [17]. It is based on the MIRD formalism detailed in the Pamphlet No. 17 [18]. The dose to a given target voxel k from N surrounding source voxels h (including dose contributions from the target voxel itself, $h=0$) can be summarized by the equation (3):

$$D(voxel)_k = \sum_{h=0}^N \tilde{A}_{(voxel)_h} \times S(voxel_k \leftarrow voxel_h) \quad (3)$$

where $\tilde{A}_{(voxel)_h}$ is the time-integrated activity (TIA) within voxels h and $S(voxel_k \leftarrow voxel_h)$ is the absorbed dose per unit cumulated activity between each voxel.

This was implemented in the dose calculation algorithm as a discrete convolution between the TIA map containing each individual $\tilde{A}_{(voxel)_h}$ and the Voxel S Value map.

Dosimetry data were then analyzed using EBRT tools: dose distribution with isodose display and dose volume histogram (DVH).

2.2.4. Treatment

The treatment consisted in the intra-arterial injection of 2619 MBq of ^{90}Y -loaded resin microspheres (SIR-Spheres[®], SIRTech Medical, North Sydney, Australia). Residual activity was measured by the pharmacist and was estimated to 1.93%. Microsphere distribution was controlled by a PET/CT exam on the next day. PET/CT acquisition of 1 bed (20 min) was done on a Biograph mCT (Siemens Healthcare, Erlangen, Germany). The PET reconstruction parameters used for SIRT dosimetry were based on the QUEST study by Willowson *et al.* [19]: True X + time of flight reconstruction algorithm (Siemens), all-pass filter, 2 iterations, 21 subsets, matrix 200 x 200, voxel size 2.04 mm x 2.04 mm x 2.03 mm.

2.2.5. Post-implantation control dosimetry

Post-treatment dosimetry was performed using the SIRT TPS. The methodology was similar to the one used for the MAA-SPECT/CT but the difference was that the activity in PET images is directly quantified in Bq/mL.

Pre and post treatment dosimetries were compared: visually in terms of dose distribution and quantitatively using DVH.

3. RESULTS

Dose results obtained by the partition model and the TPS approach described in the previous sections are summarized in Table 1. As a reminder, volumes defined by the partition model are only based on the $^{99}\text{Tc}^m$ MAA uptake whereas the volumes used in the TPS were anatomically defined on the MRI images and functionally on the MAA-SPECT exam.

3.1. Pre-implantation Dosimetry

Activity planning was based on the partition model and was adjusted with the additional information provided by the TPS with as main objective to preserve the NTL tissue. The mean dose to the NTL was close to 30 Gy whether it was calculated by the standard approach or by the 3D voxel-based calculation. In addition, the DVH provided by the TPS showed that about 60% of the NTL volume would receive less than 30 Gy (Figure 4). As described previously, the TL MAA uptake volume used for the partition model correspond to the central lesion. The mean dose value to the TL calculated by the partition model was close to the one obtained by the TPS on the anatomical central tumor (respectively $D_{TL-MAA-uptake} = 119 \text{ Gy}$ vs. $D_{Central-MAA-anat} = 115 \text{ Gy}$). Planned doses to the other lesions were evaluated using the TPS. In the clinical context of this patient, the planned dose to the gallbladder (defined anatomically) was of interest too and was estimated to 32 Gy. Doses to the MAA-uptake volumes (V_{NTL} and V_{TL}) were more or less similar for both calculation methods (organ and voxel level).

	Volumes	Mean planned dose (Gy)	Mean delivered dose (Gy)
Partition model at organ level	$V_{TL-uptake}$	119	-
	$V_{NTL-uptake}$	32	-
3D TPS at voxel level	$V_{TL-uptake}$	98	
	$V_{NTL-uptake}$	34	
	$V_{TL-anat}$	72	24
	$V_{central-anat}$	115	46
	$V_{VII-anat}$	50	14
	$V_{III-anat}$	93	153
	V_V-anat	76	7
	$V_{total\ liver-anat}$	31	28
	$V_{NTL-anat}$	30	28
	$V_{Gallbladder-anat}$	32	14

Table 1: Dose results for the partition model (organ level) and for the 3D TPS calculation (voxel level). The planned dose was calculated prior to the treatment based on the MAA-SPECT scan while the *in vivo* delivered dose was calculated by the TPS on the ^{90}Y -PET scan. As a reminder, $V_{TL-anat}$ was the sum of the 4 lesions whereas $V_{TL-uptake}$ was defined on the central lesion uptake; $V_{NTL-uptake}$ was defined as $V_{IL-uptake} - V_{TL-uptake}$ whereas $V_{NTL-anat}$ was defined as $V_{total\ liver-anat} - V_{TL-anat}$.

3.2. In vivo Control vs. Planning Dosimetry

Compared to the $^{99}\text{Tc}^{\text{m}}$ -labeled MAA, the distribution of ^{90}Y -loaded microspheres was visually very poor in the right liver and was preferential in the left liver. Real delivered doses were only calculated by the TPS using the ^{90}Y quantified PET images. The mean delivered dose to the NTL was close to what was expected. Moreover, about 70% of the NTL volume received less than 30 Gy. For the TL, the mean delivered dose to the anatomical central lesion was much lower than predicted ($D_{\text{central-90Y-anat}} = 46 \text{ Gy}$ vs. $D_{\text{central-MAA-anat}} = 115 \text{ Gy}$). The same trend was observed for the tumors of the segment VII and V. On the contrary, mean dose delivered to the lesion of the segment III was higher than expected ($D_{\text{III-90Y-anat}} = 153 \text{ Gy}$ vs. $D_{\text{III-MAA-anat}} = 93 \text{ Gy}$). The gallbladder received about twice less dose than what was expected from the MAA analysis.

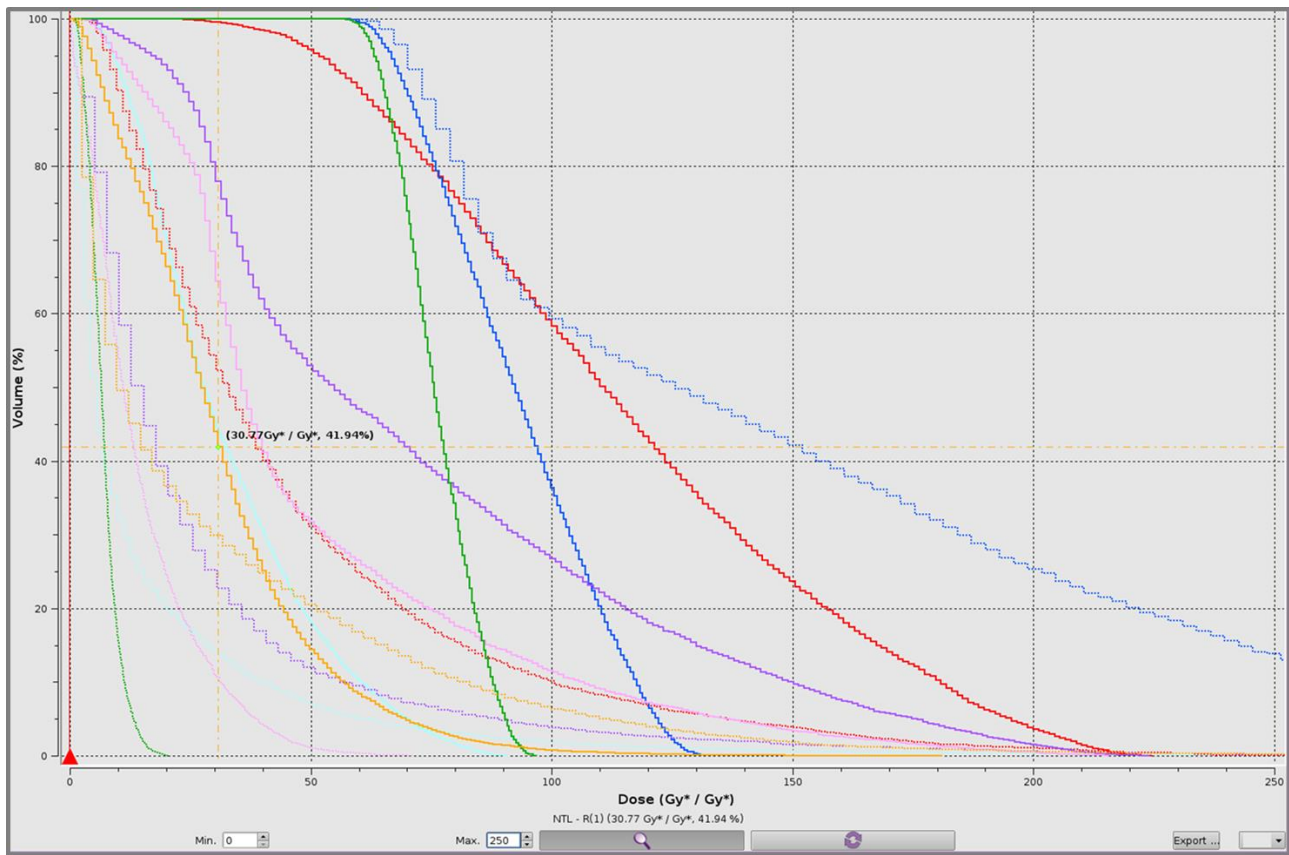


Figure 4: DVH comparing pre and post treatment dosimetries (PLANET[®] Dose, DOSIsoft). Solid lines and columns (1) of the table refer to the MAA-planning while dashed lines and columns (2) of the table refer to the *in vivo* control. Volumes represented on this DVH are: gallbladder (light blue), NTL (orange), central tumor (red), tumor III (dark blue), total tumor (purple), tumor VII (pink), tumor V (green).

4. DISCUSSION

Dosimetry for this patient was assessed by two different methods. Differences in terms of planned dose were additionally to the different calculation method related to the volume definition. Only the central lesion was included in the MAA-uptake volume used as TL in the standard approach while the anatomical TL was composed of the four lesions. In the case described here, the TL uptake volume was defined in this way in the standard approach to get an initial activity estimation on the central

lesion which was then adapted with the additional information provided by the TPS. This was a good example to show that the partition model used so far can be easily and efficiently applied when the uptake volume matches well the anatomical volume but has some limitations otherwise. The small difference (4 Gy) between the doses calculated to the MAA-uptake NTL volumes ($V_{TL-uptake}$) by the 2 methods is mainly due to the isocontour method used. In the TPS, the isocontour can be limited to the anatomical boundaries of the liver volume so that lung or extrahepatic uptake cannot be taken into account in the delineated volume.

In vivo dosimetry was not performed using the standard approach because of the complicated delineation of volumes on the ^{90}Y PET exam due to the low signal, the intrinsic noise and the availability of delineation tools apart from the isocontouring method.

Qualitative deviations between $^{99}\text{Tc}^m$ -labeled MAA and ^{90}Y -loaded microspheres distributions were quantitatively confirmed by 3D TPS pre and post treatment dosimetry comparison. These differences could be explained by the operating differences observed during the therapeutic intervention. Before injecting the microspheres the interventional radiologist temporarily embolized the cystic artery to preserve the gallbladder. Besides, a vasospasm of the right hepatic artery occurred making the microsphere flow go preferentially to the left liver.

In addition to the mean planned and delivered dose values to the NTL, the DVH was helpful to evaluate that about 60% of the volume was planned to receive less than 30 Gy and that about 70% actually received less than 30 Gy. This can be explained by the NTL volume as defined for this patient case that includes a part of the perfusion volume and the non-target liver as well.

The patient had a MRI control exam 2 months after the injection of microspheres. Compared with the diagnostic MRI, lesions were on average stable with a slight size increase for the lesions of the right liver and a slight size decrease for the lesions of the left liver. Moreover, the patient got a radiation hepatitis in the left liver. These results are compliant with the *in vivo* dosimetry.

Due to their small size, the lesions V (2 mL) and III (3 mL) are significantly affected by the partial volume effect. This should be taken into account in the ^{90}Y DVH analysis and will be corrected for future analysis with the recovery coefficients calculated in accordance with Willowson *et al.* paper [19].

Although the treatment did not happen like expected, ^{90}Y dosimetry allowed to quantify the real delivered dose to each volume of interest (lesions, NTL and gallbladder) for the patient follow-up and to possibly consider another treatment (second radioembolization or other therapy).

Other patient cases were studied retrospectively and prospectively. In addition to dosimetry optimization like in EBRT, using a 3D TPS for SIRT highlighted other advantages.

For planning purpose, when the LSF was significant, 3D estimation of this factor (which is one of the constraints of this treatment technique) is quantitatively more precise than the planar image analysis that does not take into account scatter and diffusion corrections and that is based on inaccurate contours.

The TPS allows activity assessment in the ^{90}Y PET field of view and per volume of interest. In two cases studied so far, post-treatment dosimetry highlighted significant differences with the planning

one related to the delivered activity that was lower than expected. This could be hardly quantified with the standard process.

3D dosimetry proved to be particularly interesting in the case of multiple small uptakes that would not be easily and accurately evaluated with the isocontour method.

The question of NTL volume definition to assess liver toxicity will also be studied. When the injection is not in the whole liver, toxicity volume will be defined as the subtraction “perfusion volume – anatomical TL”.

Implementing a new system for SIRT planning and *in vivo* control not only help the department regarding the dosimetry analysis but also gathering the expertise of each medical field.

This paper aimed at describing a new methodology for SIRT dosimetry through a unique example. Dose-effect relationship will be studied on a large number of patients to improve this methodology and identify the relevant dosimetry parameters to be analyzed and taken into account for this therapy.

5. CONCLUSION

SIRT TPS seemed to be a clinical decision-making tool thanks to the possible risk/benefit balance optimization. This can be especially interesting for patients with limited liver integrity. It can also help assessing dose to anatomical tumors which are sometimes partially targeted. The study will be carried out with further patients to open the way to more personalized SIRT dosimetry.

REFERENCES

- [1] M. Cremonesi, C. Chiesa, L. Strigari, et al., “Radioembolization of hepatic lesions from a radiobiology and dosimetric perspective”, *Front Oncol*, **4**:210 (2014).
- [2] RG. Selwyn, RJ. Nickles, BR. Thomadsen, LA. DeWerd, JA. Micka, “A new internal pair production branching ratio of ^{90}Y : the development of a non-destructive assay for ^{90}Y and ^{90}Sr ”, *Appl Radiat Isot*, **65**, pp.318–27 (2007).
- [3] A. Kennedy, D. Coldwell, B. Sangro, et al., “Radioembolization for the treatment of liver tumors general principles”, *Am J Clin Oncol*, **35**, pp.91-99 (2012).
- [4] B. Sangro, R. Salem, A. Kennedy, et al., “Radioembolization for hepatocellular carcinoma: a review of the evidence and treatment recommendations”, *Am J Clin Oncol*, **34**, pp. 422-31 (2011).
- [5] R. Murthy, P. Kamat, R. Numez, et al. “Radioembolization of yttrium-90 microspheres for hepatic malignancy”, *Semin Intervent Radiol*, **25**, pp.48-57 (2008).
- [6] C. Breedis C, G. Young. “The blood supply of neoplasms in the liver”, *Am J Pathol*, **30**, pp.969-84 (1954).
- [7] MA. Burton, B. Gray, PF. Klemp, DK. Kelleher, N. Hardy, “Selective Internal Radiation Therapy: Distribution of radiation in the liver”, *Eur J Cancer Clin Oncol*, **25**, pp.1487-91 (1991).
- [8] AF. Van den Hoven, C. Rosenbaum, SG. Elias et al., “Insights into the dose-response relationship of radioembolization with resin yttrium-90 microspheres: a prospective cohort study in patients with colorectal can liver metastases”, *J Nucl Med*, **57**, pp.1014-19 (2016).
- [9] E. Garin, L. Lenoir, Y. Rolland, J. Edeline, H. Mesbah, S. Laffon, et al., “Dosimetry based on $^{99\text{m}}\text{Tc}$ -macroaggregatd albumin SPECT/CT accurately predicts tumor response and survival in hepatocellular carcinoma patients treated with ^{90}Y -loaded glass microspheres: preliminary results”, *J Nucl Med*, **53**, pp.255-63 (2012).

- [10] YH. Kao, JD. Steinberg, YS. Tay, GK. Lim, J. Yan, DW. Townsend, et al. “Post-radioembolization yttrium-90 PET/CT - part 2: dose-response and tumor predictive dosimetry for resin microspheres”, *EJNMMI Res*, **3**, pp.559-66 (2013).
- [11] S. Ho, WY. Lau, TW. Leung, M. Chan, PJ. Johnson, AK. Li, “Clinical evaluation of the partition model for estimating radiation doses from yttrium-90 microspheres in the treatment of hepatic cancer”, *Eur J Nucl Med*, **24**, pp.293-8 (1997).
- [12] JM. Campbell, CO. Wong, O. Muzik, B. Marples, M. Joiner, J. Burmeister, “Early dose response to yttrium-90 microsphere treatment of metastatic liver cancer by a patient-specific method using single photon emission computed tomography and positron emission tomography”, *Int J Radiat Oncol Biol Phys*, **74**, pp.313-20 (2009).
- [13] L. Strigari, R. Sciuto, S. Rea, L. Carpanese, G. Pizzi, A. Soriani, et al., “Efficacy and toxicity related to treatment of hepatocellular carcinoma with ⁹⁰Y-SIR spheres: radiobiologic considerations”, *J Nucl Med*, **51**, pp.1377-85 (2010).
- [14] P. Flamen, B. Vanderlinden, P. Delatte, G. Ghanem, L. Ameye, M. Van Den Eynde, et al., “Multimodality imaging can predict the metabolic response of unresectable colorectal liver metastases to radioembolization therapy with yttrium-90 labeled resin microspheres”, *Phys Med Biol*, **53**, pp.6591–603 (2008).
- [15] E. Garin, Y. Rolland, L. Lenoir, et al. “Utility of quantitative Tc-MAA SPECT/CT for yttrium-labelled microsphere treatment planning: calculating vascularized hepatic volume and dosimetric approach”, *Int J Mol Imaging*, **53**, pp.255-263(2011).
- [16] R. Loevinger, TF. Budinger, EE. Watson, *MIRD primer for absorbed dose calculations. Revised*. The Society of Nuclear Medicine, New York, NY, USA (1991).
- [17] A. Dieudonne, RF. Hobbs, WE. Bolch, G. Sgouros, I. Gardin, “Fine-resolution voxel S values for constructing absorbed dose distributions at variable voxel size”, *J Nucl Med*, **51**, pp.1600-07 (2010).
- [18] WE. Bolch, LG. Bouchet, JS. Robertson, et al., “MIRD pamphlet No. 17: the dosimetry of nonuniform activity distributions—radionuclide S values at the voxel level”, Medical Internal Radiation Dose Committee, *J Nucl Med*, **40** (1999).
- [19] KP. Willowson, M. Tapner, DL. Bailey, The QUEST Investigator Team, “A multicentre comparison of quantitative ⁹⁰Y PET/CT for dosimetric purposes after radioembolization with resin microspheres”, *Eur J Nucl Med Mol Imaging*, **42**, pp.1202-1222 (2015).